

Electronic and electrochemical properties of grid-type metal ion complexes (Fe²⁺ and Co²⁺) with a pyridine-pyrimidine-pyridine based bis(hydrazone)

Abstract

The synthesis of new grid-type complexes of Co²⁺ and Fe²⁺ based on a highly soluble double hydrazone framework is reported. The data obtained from ¹H NMR, FT-IR, and elemental analysis indicate that the complexes adopted a grid-like structure. Electronic properties of the metallogrids were analyzed by UV-Vis spectroscopy in chloroform, methanol, and dichloromethane. Additionally, cyclic voltammetry and square wave voltammetry were carried out in N,N-dimethylformamide (DMF). These compounds exhibited two oxidation processes corresponding to the organic ligand and several reductions events, comprising the ligand and metal centers. Furthermore, the interplay between the metal nature and the ligand framework was also studied in detail. These results represent an advancement in the chemistry of metallogrids not only because of the few reports concerning to the electrochemical properties found in the literature, but also for the design of novel hydrazone ligands of high solubility and easy preparation.

Keywords: bis(hydrazones); electrochemistry; metallogrids; supramolecular chemistry.

Propiedades electrónicas y electroquímicas de complejos metálicos (Fe²⁺ y Co²⁺) tipo rejilla con una bis(hidrazona) con estructura piridina-pirimidina-piridina)

Resumen

Se reporta la síntesis de nuevos complejos metálicos de Co²⁺ y Fe²⁺ tipo rejilla que contienen como ligando orgánico una doble hidrazona altamente soluble en solventes orgánicos. Los datos obtenidos de resonancia magnética nuclear (RMN ¹H), espectroscopía infrarroja con transformada de Fourier (FT-IR) y análisis elemental indican que los complejos adoptaron una estructura de tipo rejilla. Las propiedades electrónicas de las metalo-rejillas fueron analizadas a través de espectroscopía UV-Vis en cloroformo, metanol y diclorometano. Adicionalmente, se realizaron medidas de voltamperometría cíclica y voltametría de onda cuadrada en DMF. Los complejos exhibieron dos procesos de oxidación atribuidos al ligando orgánico y a varios eventos reductivos que comprometían al ligando y a los centros metálicos, por tanto, la interacción entre la naturaleza del ion metálico y la estructura del ligando fue analizada en detalle. Estos resultados representan un avance en la química de metalo-rejillas no solo por los escasos reportes de propiedades electroquímicas encontrados en la literatura, sino también por el diseño de nuevos ligandos hidrazónicos de alta solubilidad y fácil preparación.

Palabras clave: bis(hidrazonas); electroquímica; metalorrejillas; química supramolecular.

Propriedades eletrônicas e eletroquímicas dos complexos metálicos (Fe²⁺ e Co²⁺) tipo grelha com uma bis(hidrazona) baseada em uma estrutura de piridina-pirimidina-piridina

Resumo

Neste trabalho relata-se a síntese de novos complexos de Co²⁺ e Fe²⁺ tipo grelha baseados na estrutura de uma hidrazona dupla altamente solúvel em solventes orgânicos. Os dados obtidos de ressonância magnética nuclear (¹H RMN), espectroscopia de infravermelho com transformada de Fourier (FT-IR), e análise elemental indicam que os complexos adotaram a estrutura tipo grelha. As propriedades eletrônicas das grelhas metálicas foram analisadas por espectroscopia UV-Vis em clorofórmio, metanol e diclorometano. Adicionalmente, foram realizadas medidas de voltametria cíclica e voltametria de onda quadrada em DMF. Os compostos estudados exibiram dois processos de oxidação correspondentes ao ligando orgânico, e a vários eventos reductivos que envolvem o ligando orgânico e os centros metálicos. Além disso, a interação entre a natureza do metal e a estrutura do ligando foi estudada em detalhe. Estes resultados representam um avanço na química de metalo-grelhas não somente pelos escasos relatos de propriedades eletroquímicas encontrados na literatura, mas também pelo design de novos ligandos hidrazônicos de alta solubilidade e fácil preparação.

Palavras-chave: bis(hidrazonas); eletroquímica; metalo-grelhas; química supramolecular.

Introduction

Supramolecular chemistry was defined by Jean-Marie Lehn (Nobel Prize in Chemistry 1987) as “The chemistry beyond the molecule” (1-5), where non-covalent interactions are responsible for holding together the supramolecular entities and building, by self-assembly, more complex architectures (1). In this regard, nature and specifically biological systems have been a great inspiration to supramolecular chemists (6, 7) making use of intramolecular interactions to replicate biological systems, to develop new applications in medicine (8), to design and synthesize drug delivery systems (9), and to develop molecular machines (10), self-healing materials (11), among others (1, 5, 12).

One of the most attractive interactions for supramolecular chemistry has been metal-ligand coordination interactions and receptor-host systems. The pioneering research has been developed by Pedersen and Cram in crown ethers (13, 14) and by Lehn in Cryptands (15, 16). More elaborated metal-supramolecular systems such as catenanes (17, 18), molecular knots (19), metal-cages (20), and metallogrids (21) have been reported. The latter have aroused great interest in the scientific community for their potential electronic properties and the possibility to exhibit spin-crossover phenomena that could convert them into storage information devices and magnetic nanodevices which are able of modulating their spin states by thermic or optical excitation (24).

The first reports on metallogrids synthesis included preparations from polytopic linear organic ligands, that is, with at least two tridentate (terpyridine) or bidentate (bipyridine) coordination sites in their structure, that by self-assembly can coordinate metallic ions in an octahedral (if the ligand has tridentate sites) or tetrahedral (if the ligand has bidentate sites) fashion. Figure 1 shows two of the first examples found in the literature (25, 26).

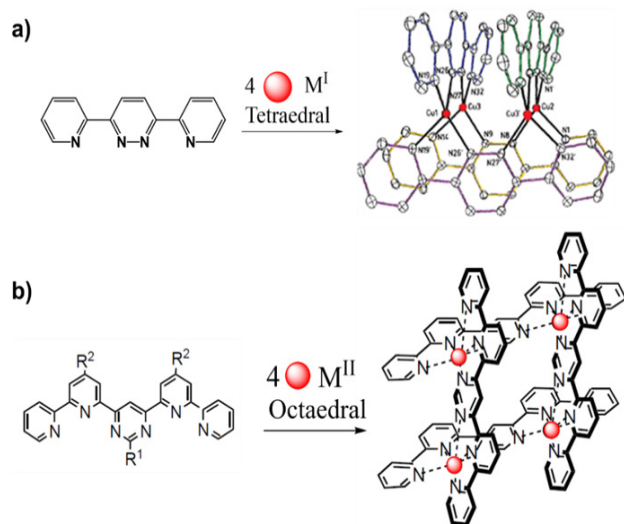


Figure 1. Formation of metallogrids based on ditopic ligands a) bipyridine and Cu⁺ ions and tritopic ligands b) terpyridine and M²⁺ ions. Image inspired by references 25 and 26.

One of the main difficulties in metallogrids formation has been the synthesis of ligands with acceptable solubility in common organic solvents. Besides, many of the synthetic protocols for preparation of terpyridine like structures imply tedious and multi-step synthesis. To overcome this issue, Lehn *et al.* (27) reported a large number of grids based in, which it turned out to be an easy preparation.

However, in many cases there is still a problem with the low solubility of hydrazones and, therefore, a restriction for the study of several of their electrochemical and spin-crossover properties. In fact, there are few reports in the literature concerning the study of electrochemical and photophysical properties of hydrazone based metallogrids (21, 23, 27).

In this work, a new bis(hydrazone) possessing a twelve carbon alkyl chain was prepared. This compound exhibited a high solubility in the majority of common organic solvents. Such bis(hydrazone) was used for the formation of Fe²⁺ and Co²⁺ metallogrids. These compounds were analyzed by ¹H NMR, elemental analysis, UV-Vis spectroscopy and cyclic and square-wave voltammetry.

Materials and Methods

All starting reagents for the synthesis of the reported compounds were purchased from Sigma-Aldrich (USA) and were used without further purification. Reactions were monitored by TLC using silica gel 60F 254 plates with a 0.2 mm thickness (Merck), manually revealed with a UV lamp Spectroline Series E with two wavelengths (254 and 365). ¹H NMR spectra were taken in a Bruker UltraShield 400 MHz instrument using CD₃CN, DMSO-*d*₆ and CDCl₃ as solvents according to the case. *E/Z* photoisomerization was carried out by UV light using a Mercury Vapor Lamp of 250 W. This process was monitored by ¹H NMR; the samples were subjected to irradiation with UV light in a quartz NMR tube. The studies were conducted in CDCl₃.

Ultraviolet spectra were taken in an UV-vis UV-1700 PharmaSpec spectrophotometer. Elemental analysis was carried out in a Thermo elemental analyzer model FlashEA 1112 CHNS; reported values are in a range of ± 0.4% of the theoretical values. The electrochemical study was registered by voltammograms in a bipotentiostat model 700B from CH Instruments.

Compound **1** and its precursors (see Figure 2) were prepared according to procedures previously reported by Lehn *et al.* (28), therefore, no additional analysis was carried out except for the ¹H NMR spectra matching.

Synthesis of 4,6-dichloro-2-(4-(dodecyloxy)phenyl)pyrimidine (2)

A solution of **1** (0.300 g, 0.72 mmol) in POCl₃ (1 mL, 10.84 mmol) was taken to reflux in an oil bath under inert atmosphere. After 8 h, 3 mL of a water-ice mixture was added, then extracted with Ethyl acetate and finally dried with sodium sulfate. After filtrating, the solvent was evaporated under reduced pressure. The resulting compound was purified using column chromatography with heptane/diethyl ether 20:1, a light yellow liquid was obtained with a 60% yield. ¹H NMR (400 MHz, chloroform-*d*) δ/ppm: 8.37 (d, J = 8.9 Hz, 2H), 7.17 (s, 1H), 6.96 (d, J = 8.9 Hz, 2H), 4.03 (t, J = 6.6 Hz, 2H), 1.85 – 1.76 (m, 2H), 1.52 – 1.43 (m, 2H), 1.41 – 1.21 (m, 16H), 0.88 (t, J = 6.8 Hz, 3H). NMR ¹³C-¹H} (101 MHz, chloroform-*d*) δ 165.75, 162.90, 161.94, 130.91, 127.40, 117.73, 114.70, 68.40, 32.08, 29.82, 29.79, 29.75, 29.72, 29.54, 29.51, 29.33, 26.17, 22.85, 14.27. Elemental analysis C 64.54 (64.52); H 7.39 (7.41); N 6.84 (6.81); O 3.91 (3.94).

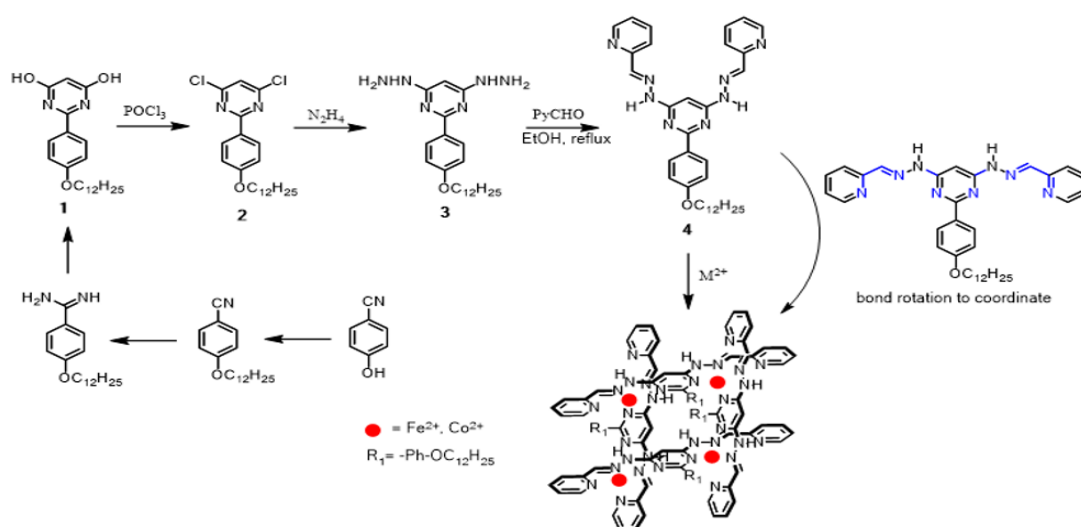


Figure 2. Synthetic route to obtain Fe(II) and Co(II) metallogrids.

Synthesis of 2-(4-(dodecyloxy)phenyl)-4,6-dihydrazinylpyrimidine (3)

Three mL of hydrazine monohydrate were added to 150 mg (0.37 mmol) of **2** under argon atmosphere. The solution was taken to reflux for 3 h, then the excess of hydrazine monohydrate was removed under reduced pressure and the product was dissolved in chloroform. The resulting solution was treated with K_2CO_3 (2 equivalents) under stirring for 10 min; the liquid phase was extracted with CHCl_3 (3 x 50 mL) and, after drying the different portions, compound **3** was obtained quantitatively as a white solid. ^1H NMR (400 MHz, $\text{DMSO}-d_6$) δ 8.18 (d, $J = 8.7$ Hz, 2H), 7.48 (s, 2H), 6.92 (d, $J = 9.1$ Hz, 2H), 5.92 (s, 1H), 4.16 (s, 4H), 3.98 (t, $J = 6.5$ Hz, 2H), 1.70 (p, $J = 6.8$ Hz, 2H), 1.47 – 1.03 (m, 18H), 0.84 (t, $J = 6.6$ Hz, 3H). NMR ^{13}C - $\{^1\text{H}\}$ (101 MHz, $\text{DMSO}-d_6$) δ 166.45, 161.18, 160.09, 131.06, 129.15, 113.70, 99.63, 77.16, 67.54, 31.37, 29.10, 29.08, 29.07, 28.84, 28.78, 25.59, 22.17, 14.04. Elemental analysis C 65.97 (65.94); H 9.06 (9.01); N 20.98 (20.96); O 3.99 (4.01).

Synthesis of 2-(4-(dodecyloxy)phenyl)-4,6-bis(2-((E)-pyridin-2-ylmethylene) hydrazinyl) pyrimidine (4)

100 mg of **3** were dissolved in ethanol (3 mL) and, under inert atmosphere, an ethanolic solution of 2-pyridinecarboxaldehyde (2 equivalents, 1 mL) was added dropwise. The resulting solution was taken to reflux for 12 h. After cooling, it was recrystallized in cold ethanol. After 12 h crystals were obtained in a 79% yield. ^1H NMR (400 MHz, chloroform- d) δ 9.23 (s, 2H), 8.63 (d, $J = 4.8$ Hz, 2H), 8.32 (d, $J = 8.7$ Hz, 2H), 8.08 (d, $J = 7.9$ Hz, 2H), 8.01 (s, 2H), 7.79 (t, $J = 7.6$ Hz, 2H), 7.29 (dd, $J = 7.5, 5.1$ Hz, 2H), 7.07 (s, 1H), 6.97 (d, $J = 8.7$ Hz, 2H), 4.01 (t, $J = 6.6$ Hz, 2H), 1.80 (p, $J = 6.8$ Hz, 2H), 1.50 – 1.43 (m, 2H), 1.35 – 1.27 (m, 16H), 0.88 (t, $J = 6.8$ Hz, 3H). NMR ^{13}C - $\{^1\text{H}\}$ (101 MHz, chloroform- d) δ 162.05, 153.44, 149.69, 143.39, 136.59, 129.90, 123.88, 120.71, 114.59, 100.14, 81.55, 77.37, 68.35, 32.08, 29.82, 29.80, 29.76, 29.74, 29.56, 29.51, 29.37, 26.18, 22.85, 14.27. Elemental analysis C 70.56 (70.55); H 7.31 (7.33); N 19.36 (19.34); O 2.76 (2.79).

General procedure to obtain metallogrids

Hydrazone **4** (10 mg) was dissolved in acetonitrile (2.0 mL) under argon atmosphere. Then, a solution of acetonitrile (3.0 mL) of the respective salt, $\text{Fe}(\text{BF}_4)_2 \cdot 6\text{H}_2\text{O}$ or $\text{Co}(\text{BF}_4)_2 \cdot 6\text{H}_2\text{O}$, was added dropwise. In both cases an equivalent of the metallic ion was added with respect to the hydrazone. The resulting solution was stirred for 48 h, then concentrated to half the initial volume and 10 mL of ethyl ether were added; a black precipitate was obtained in both cases. The precipitate was dried under reduce pressure for 12 h, yielding 88% and 90% for Fe(II) and Co(II) complexes, respectively. Once dried, the solids were subject to elemental analysis and NMR. Elemental analysis: $[\text{Co}_4(1)_4](\text{BF}_4)_8 \cdot 6\text{H}_2\text{O}$ C 48.71 (48.65); H 5.41 (5.47); N 13.37 (13.30); O 4.47 (4.80). $[\text{Fe}_4(1)_4](\text{BF}_4)_8 \cdot 6\text{H}_2\text{O}$ C 48.89 (48.83); H 5.43 (5.48); N 13.42 (13.40); O 4.79 (4.82).

Results and Discussion

Synthesis of bis(hydrazone) 4

This work began with the design of a ditopic organic ligand of easy preparation and with the requirement of high solubility in common organic solvents. For that purpose, a protocol similar to the one found in the literature (19), which implied four synthetic steps towards compound **1** (See Figure 2) was carried out. This compound exhibited the same ^1H NMR signals as the one reported, therefore, no further characterization was performed (26). Subsequently, **1** was reacted with POCl_3 to obtain **2** in an 86% yield. The chloride compound was subjected to a nucleophilic aromatic substitution reaction, using hydrazine monohydrate as solvent with reflux for 3 h. Excess of hydrazine was removed under reduced pressure and the obtained product was re-dissolved in chloroform. The resulting solution was treated with K_2CO_3 (2 equivalents) under constant stirring for 10 min. The liquid phase was extracted with CHCl_3 (3 x 50 mL) and the extracts were taken to dryness obtaining compound **3** quantitatively as a white solid. This compound proved to be sensitive to air and had to be used as soon as possible in the following reaction because it tended to decompose into a black substance, which was insoluble in common organic solvents.

Once compound **3** was obtained, it was dissolved in ethanol and added dropwise to an ethanolic solution of 2 equivalents of 2-pyridinecarboxaldehyde. The resulting solution was taken to reflux for 12 h. After cooling, compound **4** was recrystallized in cold ethanol (after ~12 h crystallization begins) and compound **4** in a 79% yield as a beige solid soluble in ethanol, methanol (partially), chloroform, DMSO, acetonitrile, dichloromethane, DMF, acetone, nitromethane, THF, and ethyl acetate, was obtained. Figure 3 shows ^1H NMR spectra of compounds **2**, **3** and **4** which, to the best of our knowledge, have not been reported in literature. Compound **4** is a new type of organic ligand, which can be seen as two arms system whose *transoid*-conformation is capable of, via two bonds rotation, change to a *cisoid*-conformation and coordinate metallic ions through the nitrogen atoms of the pyrimidine, imine and pyridine moieties, acting similar to a terpyridine ligand (Figure 2). Through such coordination molecular metallogrids of high solubility can be obtained, allowing the study of electronic and electrochemical properties as it is reported in the present work.

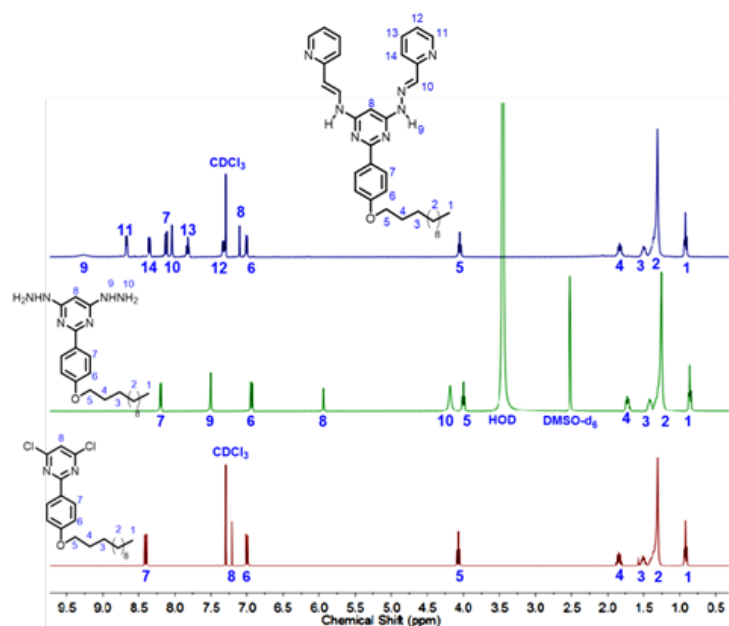


Figure 3. ^1H NMR (400 MHz) spectra expansion of compounds **2** (in CDCl_3), **3** (in $\text{DMSO}-d_6$) and **4** (in CDCl_3).

Compounds **2**, **3**, and **4** showed the right number of characteristic signals of each molecule. At high field, four signals integrate for 23 protons, which correspond to those of the alkyl chain. Besides, around 4.0 ppm a triplet integrating for two protons was observed. This triplet corresponded to the methyl group bonded directly to oxygen. As expected, the signals of the alkyl chain were not affected by the substitution occurring in the pyrimidine ring and, therefore, they were observed at similar chemical shifts in the three compounds. At downfield the protons corresponding to the aromatic rings were seen. For the case of **2**, two doublets (8.37 and 6.96 ppm, $J = 8.90$), which corresponded to the protons of the aromatic ring, are bonded to the pyrimidine center. Furthermore, there was a singlet at 7.17 ppm integrating for one proton corresponding to H-5 in the pyrimidine ring. In the case of **3**, additionally to signals observed for **2**, there were two new signals at 7.50 and 4.18 ppm integrating for two and four protons corresponding to the two of hydrazone units, respectively.

For the case of bis(hydrazone) **4**, five additional signals correspond to the imine group protons and those of the pyridine ring. All the signals integrated correctly. The two N-H protons appeared as a wide band due to the rapid proton exchange in solution.

The ^{13}C NMR spectrum showed the 25 expected signals, 14 of which appear at downfield and correspond to aromatic carbons and the alpha carbon to oxygen. At high field (14-32 ppm) there were 11 signals corresponding to the alkyl chain. The HSQC (Figure 4) allows the assignment of the corresponding signals.

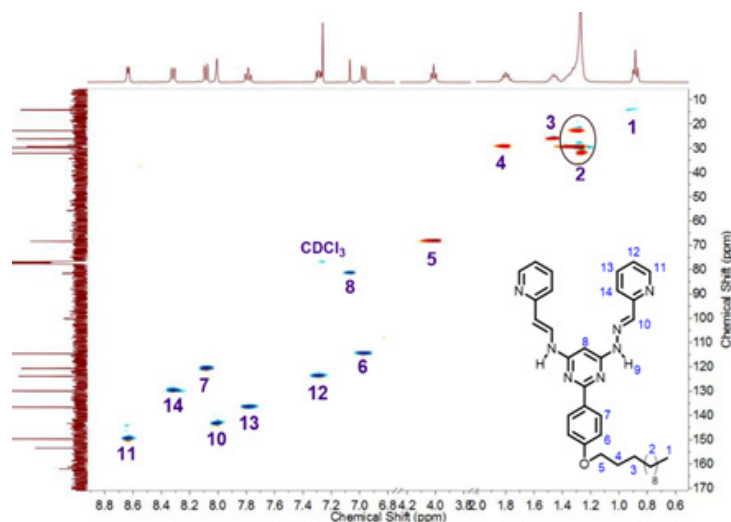


Figure 4. HSQC spectrum (400 MHz) of bis(hydrazone) **4** in CDCl_3 .

Formation of metallogrids

Once prepared the bis(hydrazone) **4**, the formation of Fe(II) and Co(II) metallogrids was carried out. Such compounds were prepared through a self-assembly process between hydrazone and M^{2+} ions ($\text{M} = \text{Fe}$ or Co) at room temperature. The elemental analysis for structures $[\text{Co}_4(\mathbf{4})_4](\text{BF}_4)_8 \cdot 6\text{H}_2\text{O}$ and $[\text{Fe}_4(\mathbf{4})_4](\text{BF}_4)_8 \cdot 6\text{H}_2\text{O}$ agreed well with the theoretical values (Table 1). This result is proof of the thermodynamic stability of the metallogrids and how these are the product of the self-assembly of several molecular components by molecular cooperativity (21, 29).

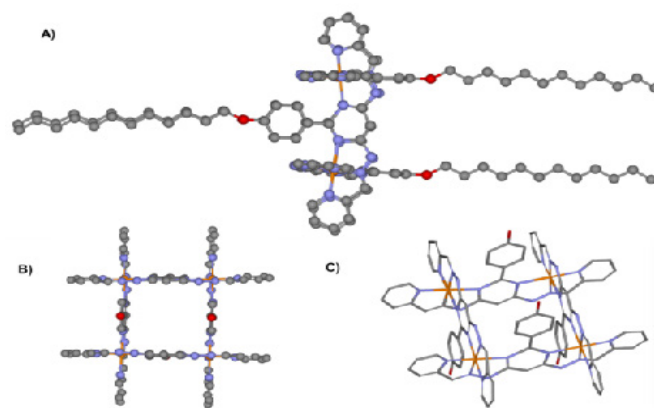


Figure 5. A) Computed structure of metallogrids of **1**. B) and C) top and side view of the metallogrids; for simplicity, alkyl chains were removed. Carbon atoms are represented in grey, oxygen in red, nitrogen in blue and metallic ions in orange.

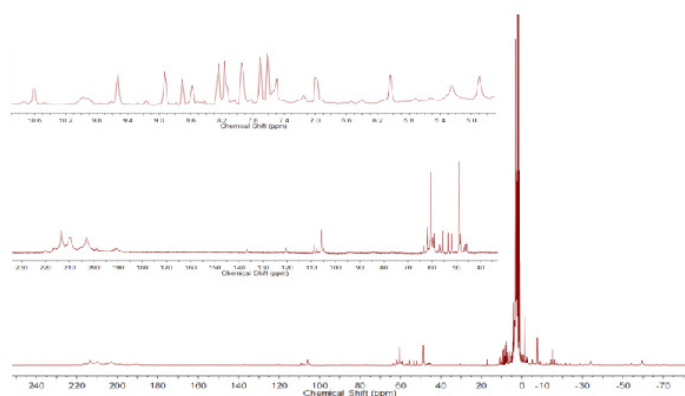
Table 1. Theoretical and experimental values of the elemental analysis of synthesized metalloids.

Compound	%C	%H	%N	%O
[Co ₄ (4) ₄](BF ₄) ₈ ·6H ₂ O (21, 29)	48.71	5.41	13.37	4.77
Experimental	48.65	5.47	13.30	4.80
[Fe ₄ (4) ₄](BF ₄) ₈ ·6H ₂ O (21, 29)	48.89	5.43	13.42	4.79
Experimental	48.83	5.48	13.40	4.82

Figure 5 shows how four molecules of bis(hydrazone) and four metallic centers are organized. The M²⁺ cations coordinate octahedrally to six nitrogen atoms from two perpendicular bis(hydrazones). The four alkyl chains are orientated outside the metallogrid.

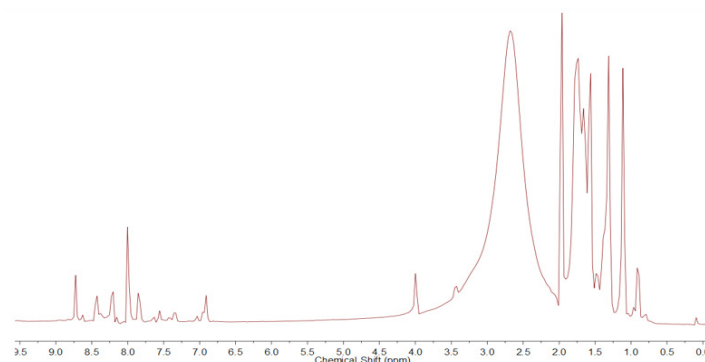
¹H NMR of metalloids

The obtained metalloids were analyzed by ¹H NMR in deuterated acetonitrile (Figures 5 and 6). In the case of Co(II) metallogrid, a paramagnetic complex is obtained with signals from -60 to 220 ppm. The large number of signals were interesting because they indicate that not all the metallic centers had the same spin and, thus, the protons of the four bis(hydrazones) were not equivalent. The same phenomena has been observed in other metalloids and coordination complexes previously published. It has been largely attributed to the influence exerted by the Co(II) ions over the local magnetic field and to the relaxation rate of protons (30-35).

**Figure 6.** ¹H NMR (400 MHz) spectra of Co(II) metallogrid in deuterated acetonitrile. Concentration 50 mM.

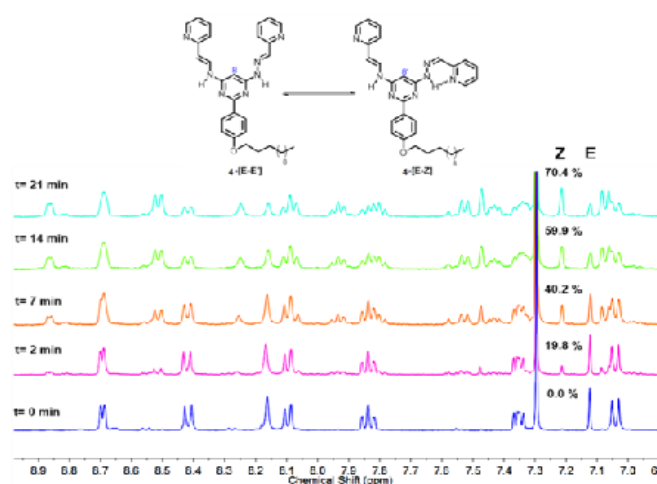
In the case of Fe(II) complex, wide signals were observed. However, these were not localized over a broad range of chemical shift as it was obtained for the Co(II) counterpart. This suggests that the metallogrid is under low/high spin crossover, as it was also observed by Lehn *et al.* (34-37). However, although supported by the literature, this assertion will keep being a conjecture until Mössbauer spectroscopy, Light-Induced Excited Spin-State Trapping (LIESST) and thermomagnetic experiments can be carried out. In this regard, paramagnetism in metalloids can occur for at least four reasons:

1) inter and intramolecular steric effects of the ligands (38-39), 2) electronic effects of the ligands and their substituents (40-42), 3) protonation state of the ligand (43), and 4) the type of counterion of the grid (44-45). All these factors affect in different degrees the magnetic properties of the metalloids and, thus, its ability to exhibit the spin crossover phenomena (25).

**Figure 7.** ¹H NMR (400 MHz) spectrum of Fe(II) metallogrid in deuterated acetonitrile. Concentration 50 mM.

E/Z photoisomerization

To follow the occurrence of isomers in the Z and E configurations, a 100.0 mM solution of 4-E,E in CDCl₃ was prepared and introduced in a quartz NMR tube, which was irradiated with a mercury vapor lamp of 250 W for different times, varying between 0 to 21 min. The photoisomerization was monitored by ¹H NMR spectroscopy to quantify the amounts of the formed isomers. When examining the ¹H NMR spectrum, the singlet at 7.13 ppm, corresponding to the 8-proton on the structure, split as the isomers were formed, indicating the formation of intramolecular hydrogen bonds. Photoisomerization was monitored over time and the relative amounts of each isomer were calculated (see Figure 8) and used to determine a first order reaction with a kinetic constant $k = 9.5 \times 10^{-4} \text{ s}^{-1}$. The percentages of the E,E' and E,Z isomers were 29.6 and 70.4% respectively, after irradiating the sample during 21 min. No Z,Z was observed during this time window.

**Figure 8.** Photoisomerization of 4. Top: Scheme of photochemically activated isomerization. Bottom: ¹H NMR (400 MHz) spectrum of bis(hydrazone) 4 in CDCl₃ at different irradiation times in a quartz tube.

Electronic studies (UV-Vis)

Methanol, chloroform, and dichloromethane solutions of the bis(hydrazone) and its metallogrids were analyzed by UV-Vis spectroscopy. Figure 9 shows the spectra in methanol and Table 2 the characteristic absorptions.

For the bis(hydrazone) **4** a very intense band was observed at 303 nm with a shoulder at 334 nm. This absorption is associated to a $\pi \rightarrow \pi^*$ electronic transition which exhibited a hypochromic shift when reducing the polarity of the solvent. The same transitions were observed for Fe(II) and Co(II) complexes but with lower intensities. Besides, additional absorption bands were detected in the visible region of the spectra, which are attributed to $d \rightarrow d$ transitions.

Table 2. UV-Vis bands in methanol associated to the compounds presented in this work.

Compound	Wavelength (nm)
Bis(hidrazone)	516 and 447 low intensity; 334 (shoulder), 303, 238, and 220
$[\text{Co}_4(\mathbf{4})_4](\text{BF}_4)_8$	528, 412 (low intensity), 304 (wide with a non-defined shoulder close to 341), 236, and 221
$[\text{Fe}_4(\mathbf{4})_4](\text{BF}_4)_8$	518, 462, 388, 349, 304, 279, 223, 208

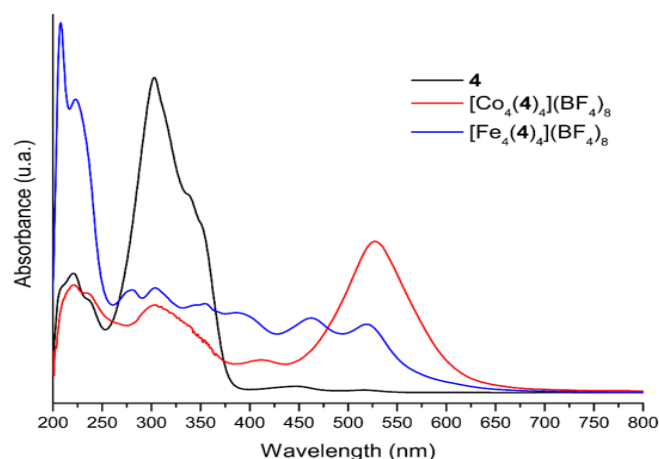


Figure 9. UV-Vis spectra of the free ligand **4** and its corresponding Fe(II) and Co(II) complexes in methanol.

In the case of the Co(II) complex, according to the NMR results, $[\text{Co}_4(\mathbf{4})_4](\text{BF}_4)_8$ corresponds to a (d^7) complex of high spin (low field). Therefore, ${}^4T_{1g}(F) \rightarrow {}^4T_{2g}$, ${}^4T_{1g}(F) \rightarrow {}^4A_{2g}$, and ${}^4T_{1g}(F) \rightarrow {}^4T_{2g}(P)$ transitions were expected. The last two are of high energy (according to Tanabe-Sugano diagram) and thus they are not observable within the measured window. The $d-d$ transitions exhibit Jahn-Teller distortions in dichloromethane, probably due to the interactions of the solvent with the organic ligands, which are evident because of the hypochromic shift, increasing the solvent polarity (Figure 10). By contrast, the Fe(II) (d^6) complex exhibited only one ${}^5T_{2g}(D) \rightarrow {}^5E_g$ allowed transition. However, in methanol an additional electronic transition was observed, which is likely due to formation of a complex (*via* hydrogen bond) between the solvent and the metallogrid.

Electrochemical Studies

Cyclic and squared wave voltammetry studies were carried out for ligand **4** and its corresponding metallogrids, in 0.1 M solutions of NBu_4PF_6 in DMF. A 3 mm glassy carbon electrode was used as working electrode, a silver wire as pseudo-reference electrode, and a wire of platinum as a counter electrode. Ferrocene was added at the end of the experiment and its oxidation potential was taken as internal reference.

Bis(hydrazone) **4** exhibited two irreversible oxidative processes, which shift slightly towards cathodic potentials after coordination with Fe(II) and Co(II). These oxidations are probably located at the $-\text{N}-\text{H}$ moiety of the hydrazone framework (46). The inherent acidity of the N-H protons facilitates the oxidative process. However, the relative oxidation potentials do not seem to be affected by the metal ion present in the complex, suggesting that the central pyrimidine group would play an active role during the oxidation mechanism (47, 48).

Besides that, compound **4** exhibited five irreversible reduction potentials, going from -1.10 V until -2.54 V. When comparing with other reports, these potentials can be attributed to reduction of the imine groups from the hydrazone framework and the lateral pyridines. Such reduction potentials were also observed for Fe(II) and Co(II) complexes and have been summarized in Table 3. In the case of Co(II) metallogrid, two additional reductions were observed, presumably due to the reduction processes in the metallic centers. Whereas for Fe(II) metallogrid only one additional reduction was observed.

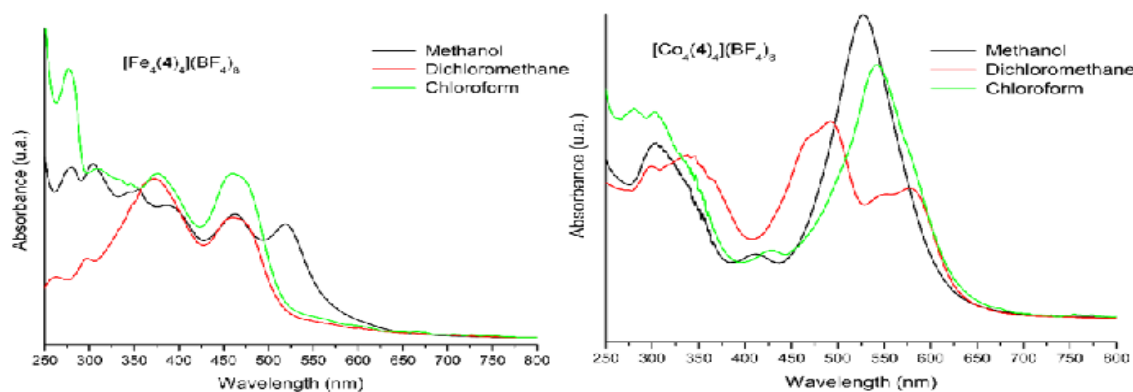


Figure 10. UV-Vis spectra of Fe(II) (left) and Co(II) (right) metallogrids in methanol, dichloromethane and chloroform.

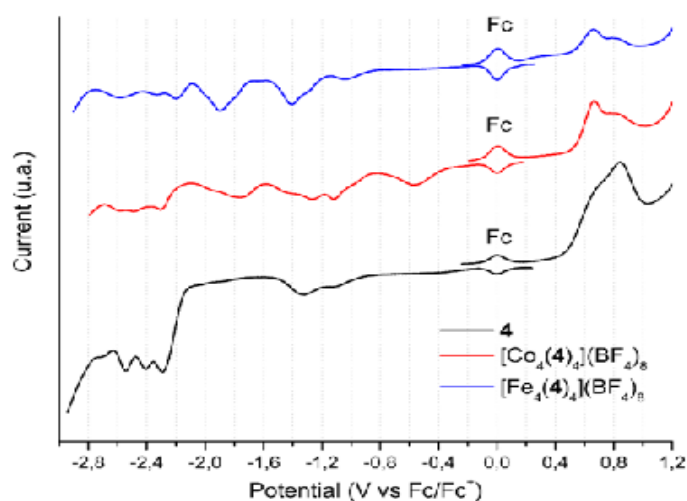


Figure 11. Squared wave voltammetry of the bis(hydrazone) **4** (in black) and Fe^{2+} (in blue) y Co^{2+} (in red) metallogrids. Scan rate 100 mV s^{-1} .

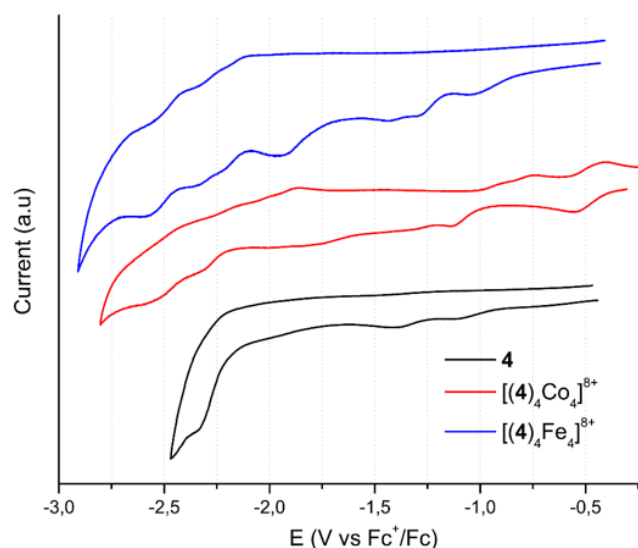


Figure 12. Cyclic voltammetry of the bis(hydrazone) **4** (in black) and Fe^{2+} (in blue) y Co^{2+} (in red) metallogrids. Scan rate 100 mV s^{-1} .

In general, these compounds exhibit electrochemistry mainly characterized by processes occurring on the hydrazone framework (amine or imine groups). It is interesting that oxidation of Fe(II)/Fe(III) was not observed, probably because of a shielding effect of the hydrazones which anodically shifts such process. Noteworthy, these compounds exhibit multiple reduction states, which can be further studied, along with the above mentioned paramagnetic properties, for the development of multi-responsive devices (49).

Table 3. Anodic and cathodic potentials of bis(hydrazone) **1** and its complexes. Potentials reported in volts vs ferrocene.

Compound	Ep, oxd(1)	Ep, oxd(2)	Ep, red(1)	Ep, red(2)	Ep, red(3)	Ep, red(4)	Ep, red(5)	Ep, red(6)	Ep, red(6)
4	0.67	0.84	-1.10	-1.32	-2.29	-2.40	-2.54		
$[\text{Co}_4(\mathbf{4})_4](\text{BF}_4)_8$	0.66	0.79	-0.57	-1.11	-1.27	-1.77	-2.30	-2.48	-2.58
$[\text{Fe}_4(\mathbf{4})_4](\text{BF}_4)_8$	0.66	0.80	-1.03	-1.40	-1.89	-2.20	-2.33	-2.58	

Conclusions

A new ditopic ligand based on a double hydrazone was prepared. This compound contains two terpyridine-like tridentate coordination sites, which are capable of forming metallogrids with Fe(II) and Co(II) ions. Such metallogrids exhibited high spin for the Co(II) complex and presumably spin-cross-over for Fe(II) metallogrids. As for the electrochemical properties of these architectures, they exhibited different irreversible cathodic process and two anodic processes mainly located at the hydrazone framework.

Acknowledgments

The authors thank the partial economic support of the Center for Excellence in new Materials, CENM and Vicerrectoria de Investigaciones from Universidad del Valle for their financial support to carry out this research. Thanks are due to Prof. Alejandro Ortiz for lending the potentiostat for the electrochemical measures.

References

- Lehn, J. M. *Supramolecular Chemistry- Concepts and Perspectives*; Wiley-VCH Verlag GmbH & Co. KGaA: Weinheim, FRG, **1995**. DOI: <https://doi.org/10.1002/3527607439>.
- Lehn, J.-M. Programmed Chemical Systems: Multiple Subprograms and Multiple Processing/Expression of Molecular Information. *Chem. Eur. J.* **2000**, 6 (12), 2097–2102. DOI: [https://doi.org/10.1002/1521-3765\(20000616\)6:12<2097::aid-chem2097>3.0.co;2-t](https://doi.org/10.1002/1521-3765(20000616)6:12<2097::aid-chem2097>3.0.co;2-t).
- Lehn, J.-M. Toward Self-Organization and Complex Matter. *Science* **2002**, 295 (5564), 2400–2403. DOI: <https://doi.org/10.1126/science.1071063>.
- Lehn, J.-M. Toward Complex Matter: Supramolecular Chemistry and Self-Organization. *Proc. Natl. Acad. Sci.* **2002**, 99 (8), 4763–4768. DOI: <https://doi.org/10.1073/pnas.072065599>.
- Lehn, J.-M. From Supramolecular Chemistry towards Constitutional Dynamic Chemistry and Adaptive Chemistry. *Chem. Soc. Rev.* **2007**, 36 (2), 151–160. DOI: <https://doi.org/10.1039/B616752G>.
- Cragg, P. J. *Supramolecular Chemistry: From Biological Inspiration to Biomedical Applications*; Springer, **2010**. DOI: <https://doi.org/10.1007/978-90-481-2582-1>.
- Clardy, J.; Walsh, C. Lessons from Natural Molecules. *Nature* **2004**, 432 (7019), 829–837. DOI: <https://doi.org/10.1038/nature03194>.
- Faulkner, S.; Kenwright, A. M. Supramolecular Chemistry in Medicine. In *Supramolecular Chemistry*; John Wiley & Sons, Ltd: Chichester, UK, **2012**. DOI: <https://doi.org/10.1002/9780470661345.smc102>.

10. Balzani, V.; Credi, A.; Raymo, F. M.; Stoddart, J. Artificial Molecular Machines. *Angew. Chem. Int. Ed. Engl.* **2000**, *39* (19), 3348–3391. DOI: [https://doi.org/10.1002/1521-3773\(20001002\)39:19<3348::aid-anie3348>3.0.co;2-x](https://doi.org/10.1002/1521-3773(20001002)39:19<3348::aid-anie3348>3.0.co;2-x).
11. Binder, W. *Self-healing polymers : from principles to applications*; Wiley-VCH, **2013**. DOI: <https://doi.org/10.1002/9783527670185>.
12. Barboiu, M.; Stadler, A. M.; Lehn, J.-M. Controlled Folding, Motional, and Constitutional Dynamic Processes of Polyheterocyclic Molecular Strands. *Angew. Chem. Int. Ed.* **2016**, *55*, 4130–4154. DOI: <https://doi.org/10.1002/anie.201505394>.
13. Cram, D.J.; George S.H. *Organic Chemistry*. McGraw-Hill, New York. 1st ed. **1959**.
14. Pedersen, C. J. Cyclic polyethers and their complexes with metal salts. *J. Am. Chem. Soc.* **1967**, *89*(26), 7017–7036. DOI: <https://doi.org/10.1021/ja01002a035>.
15. Lehn, J.-M. Cryptates: inclusion complexes of macropolycyclic receptor molecules. *Pure Appl. Chem.* **1978**, *50*, 871–892. DOI: <https://doi.org/10.1351/pac197850090871>.
16. Lehn, J.-M. Design of organic complexing agents Strategies towards properties. *Struct. Bonding* **1973**, *16*, 1–69. DOI: <https://doi.org/10.1007/BFb0004364>.
17. Sauvage, J.-P.; Dietrich-Buchecker, C.; *Molecular catenanes, rotaxanes, and knots : a journey through the world of molecular topology*; Wiley-VCH, **1999**. DOI: <https://doi.org/10.1002/9783527613724>.
18. Gil-Ramírez, G.; Leigh, D. A.; Stephens, A. J. Catenanes: fifty years of molecular links. *Angew. Chemie Int. Ed.* **2015**, *54* (21), 6110–6150. DOI: <https://doi.org/10.1002/anie.201411619>.
19. Ayme, J.-F.; Beves, J. E.; Campbell, C. J.; Leigh, D. A.; Rissanen, K.; Schultz, D. *et al.* Template synthesis of molecular knots. *Chem. Soc. Rev.* **2013**, *42* (4), 1700–1712. DOI: <https://doi.org/10.1039/c2cs35229j>.
20. Fujita, D.; Ueda, Y.; Sato, S.; Mizuno, N.; Kumasaka, T.; Fujita, M. Self-assembly of tetravalent Goldberg polyhedra from 144 small components. *Nature*, **2016**, *540* (7634), 563–566. DOI: <https://doi.org/10.1038/nature20771>.
21. Hardy, J. G. Metallosupramolecular grid complexes: towards nanostructured materials with high-tech applications. *Chem. Soc. Rev.* **2013**, *42* (19), 7881–7899. DOI: <https://doi.org/10.1039/C3CS60061K>.
22. Fernández, M. A.; Barona, J. C.; Polo, D.; Chaur, M. N. Photochemical and electrochemical studies on lanthanide complexes of 6-(hydroxymethyl) pyridine-2-carboxaldehyde [2-methylpyrimidine-4, 6-diy] bis-hydrazone. *Rev. Colomb. Quim.* **2014**, *43* (1), 5–11. DOI: <https://doi.org/10.15446/rev.colomb.quim.v43n1.50540>.
23. Vargas, C. C. C.; Váquiro, I. Y.; Gómez, M. J.; Lehn, J.-M.; Chaur, M. N. Grid-type complexes of M^{2+} (M = Co, Ni, and Zn) with highly soluble bis(hydrazone)thiopyrimidine-based ligands: Spectroscopy and electrochemical properties. *Inorganica Chim. Acta.* **2017**, DOI: <https://doi.org/10.1016/j.ica.2017.05.002>.
24. Brooker, S. Spin crossover with thermal hysteresis: practicalities and lessons learnt. *Chem. Soc. Rev.* **2015**, *44*, 2880–2892. DOI: <https://doi.org/10.1039/c4cs00376d>.
25. Youinou, M.-T.; Rahmouni, N.; Fischer, J.; Osborn, J.A. Self-Assembly of a Cu_4 Complex with Coplanar Copper(I) Ions: Synthesis, Structure, and Electrochemical Properties. *Angew. Chemie Int. Ed.* **1992**, *31*, 733–735. DOI: <https://doi.org/10.1002/anie.199207331>.
26. Rojo, J.; Romero-Salguero, F. J.; Lehn, J.-M.; Baum, G.; Fenske, D. Self-Assembly, Structure, and Physical Properties of Tetranuclear Zn^{II} and Co^{II} Complexes of $[2 \times 2]$ Grid-Type. *Eur. J. Inorg. Chem.* **1999**, *1999*, 1421–1428. DOI: [https://doi.org/10.1002/\(sici\)1099-0682\(199909\)1999:9<1421::aid-ejic1421>3.0.co;2-j](https://doi.org/10.1002/(sici)1099-0682(199909)1999:9<1421::aid-ejic1421>3.0.co;2-j).
27. Ruben, M.; Rojo, J.; Romero-Salguero, F. J.; Uppadine, L. H.; Lehn, J.-M. Grid-type metal ion architectures: functional metallosupramolecular arrays. *Angew. Chem. Int. Ed.* **2004**, *43*, 3644–3662. DOI: <https://doi.org/10.1002/anie.200300636>.
28. Petitjean, A.; Cuccia, L. A.; Schmutz, M.; Lehn, J.-M. Naphthyridine-Based Helical Foldamers and Macrocycles: Synthesis, Cation Binding, and Supramolecular Assemblies. *J. Org. Chem.* **2008**, *73*, 2481–2495. DOI: <https://doi.org/10.1021/jo702495u>.
29. Von Krbek, L. K. S.; Schalley, C. A.; Thordarson, P. Assessing cooperativity in supramolecular systems. *Chem. Soc. Rev.* **2017**, *46*, 2622–2637. DOI: <https://doi.org/10.1039/C7CS00063D>.
30. Bertini, I.; Luchinat, C. Chapter 1, introduction. *Coord. Chem. Rev.* **1996**, *150*, 1–292. DOI: [https://doi.org/10.1016/0010-8545\(96\)01241-6](https://doi.org/10.1016/0010-8545(96)01241-6).
31. Constable, E.C.; Housecroft, C.E.; Kulke, T.; Lazzarini, C.; Schofield, E.R.; Zimmermann, Y. Redistribution of terpy ligands—approaches to new dynamic combinatorial libraries. *J. Chem. Soc. Dalton Trans.* **2001**, 2864–2871. DOI: <https://doi.org/10.1039/B104865C>.
32. Constable, E.C.; Kulke, T.; Neuburger, M.; Zehnder, M. hiral 2,2':6',2''-terpyridine ligands for metallosupramolecular Chemistry; Part 2 – metal complexes of 4'-([1S]-endo]-bornyloxy)-2,2':6',2''-terpyridine, 4'-([1R]-endo]-bornyloxy)-2,2':6',2''-terpyridine, 4'-quininyl-2,2':6',2''-terpyridine, and 4'-((2,2':6',2''-terpyridinyl)-(1S)-10-camphorsulfonate. *New J. Chem.* **1997**, *21*, 1091–1102.
33. Storrier, G.D.; Colbran, S.B.; Craig, D.C. Transition-metal complexes of terpyridine ligands with hydroquinone or quinone substituents ‡. *J. Chem. Soc. Dalton Trans.* **1998**, 1351–1364. DOI: <https://doi.org/10.1039/A709117F>.
34. Uppadine, L. H.; Gisselbrecht, J. P.; Kyritsakas, N.; Nättinen, K.; Rissanen, K.; Lehn, J.-M. Mixed-valence, mixed-spin-state, and heterometallic $[2 \times 2]$ grid-type arrays based on heteroditopic hydrazone ligands: synthesis and electrochemical features. *Chem. Eur. J.* **2005**, *11*, 2549–2565. DOI: <https://doi.org/10.1002/chem.200401224>.
35. Ramírez, J.; Stadler, A.M.; Kyritsakas, N.; Lehn, J.-M. Solvent-modulated reversible conversion of a $[2 \times 2]$ -grid into a pincer-like complex. *Chem. Commun.* **2007**, 237–239. DOI: <https://doi.org/10.1039/B612222A>.
36. Ruben, M.; Breuning, E.; Lehn, J.-M.; Ksenofontov, V.; Renz, F.; Gütllich, P.; Vaughan, G. Supramolecular Spintronic Devices: Spin Transitions and Magnetostructural Correlations in $[Fe_4^{II}L_4]^{8+}$ $[2 \times 2]$ -Grid-Type Complexes. *Chem. Eur. J.* **2003**, *9*, 4422–4429. DOI: <https://doi.org/10.1002/chem.200304933>.
37. Ruben, M.; Breuning, E.; Lehn, J.-M.; Ksenofontov, V.; Renz, F.; Gütllich, P.; Vaughan, G. Magneto-structural correlations in self-assembled spin-transition nano-architectures of the $[Fe_4^{II}L_4]^{8+}$ $[2 \times 2]$ -grid-type. *J. Magn. Magn. Mat.* **2004**, *272–276*, 715–e717. DOI: <https://doi.org/10.1016/j.jmmm.2003.12.1423>.
38. Constable, E. C.; Baum, G.; Bill, E.; Dyson, R.; van Eldik, R.; Fenske, D. *et al.* Control of Iron(II) Spin States in 2,2':6,2'-Terpyridine Complexes through Ligand Substitution. *Chem. Eur. J.* **1999**, *5*, 498–508. DOI: [https://doi.org/10.1002/\(sici\)1521-3765\(19990201\)5:2<498::aid-chem498>3.0.co;2-v](https://doi.org/10.1002/(sici)1521-3765(19990201)5:2<498::aid-chem498>3.0.co;2-v).
39. Onggo, D.; Hook, J. M.; Rae, D.; Goodwin, H. A. The influence of steric effects in substituted 2,2'-bipyridine on the spin state of iron(II) in $[FeN_6]^{2+}$ systems *Inorg. Chim. Acta.* **1990**, *173*, 19–30. DOI: [https://doi.org/10.1016/S0020-1693\(00\)91050-8](https://doi.org/10.1016/S0020-1693(00)91050-8).
40. Gütllich, P. Spin crossover in iron(II) complexes. *Struct. Bonding.* **1981**, *44*, 83–195.
41. Hathcock, D. J.; Stone, K.; Madden, J.; Slattery, S. J. Electron donating substituent effects on redox and spin state properties of iron(II) bis-terpyridyl complexes. *Inorg. Chim. Acta.* **1998**, *282*, 131–135. DOI: [https://doi.org/10.1016/S0020-1693\(98\)00154-6](https://doi.org/10.1016/S0020-1693(98)00154-6).
42. Ayers, T.; Scott, S.; Goins, J.; Caylor, N.; Hathcock, D.; Slattery, S.J.; Jameson, D.L. Redox and spin state control of Co(II) and Fe(II) N-heterocyclic complexes. *Inorg. Chim. Acta.* **2000**, *307*, 7–12. DOI: [https://doi.org/10.1016/S0020-1693\(00\)00179-1](https://doi.org/10.1016/S0020-1693(00)00179-1).

43. Enamullah, M.; Linert, W.; Gutmann, V.; Jameson, R.F. Spin-transition behaviour of transition metal complexes with 2,6-bis-(benzimidazol-2-yl)-pyridine induced by deprotonation of the complex. *Monatsh. Chem.* **1994**, *125*, 1301-1309. DOI: <https://doi.org/10.1007/BF00811079>.
44. Yamada, M.; Ooidemizu, M.; Ikuta, Y.; Osa, S.; Matsumoto, N.; Iijima, S. *et al.* Interlayer Interaction of Two-Dimensional Layered Spin Crossover Complexes [Fe^{II}H₃L^{Me}][Fe^{II}L^{Me}]X (X⁻ = ClO₄⁻, BF₄⁻, PF₆⁻, AsF₆⁻, and SbF₆⁻; H₃L^{Me} = Tris[2-(((2-methylimidazol-4-yl)methylidene)amino)ethyl]amine). *Inorg. Chem.* **2003**, *42*, 8406-8416. DOI: <https://doi.org/10.1021/ic034439e>.
45. Renovitch, G. A.; Baker Jr. W.A. Spin equilibrium in tris(2-aminomethylpyridine)iron (II) halides. *J. Am. Chem. Soc.* **1967**, *89*, 6377-6378. DOI: <https://doi.org/10.1021/ja01000a083>.
46. Adenier, A.; Chehimi, M. M.; Gallardo, I.; Pinson, J.; Vilà, N. Electrochemical oxidation of aliphatic amines and their attachment to carbon and metal surfaces. *Langmuir* **2004**, *20* (19), 8243–8253. DOI: <https://doi.org/10.1021/la049194c>.
47. Castilho, M.; Almeida, L. E.; Tabak, M.; Mazo, L. H. Voltammetric Oxidation of Dipyrindamole in Aqueous Acid Solutions. *J. Braz. Chem. Soc.* **2000**, *11* (2), 148–153. DOI: <https://doi.org/10.1590/S0103-50532000000200008>.
48. Oliveira-Brett, A. M.; Piedade, J. A. P.; Silva, L. A.; Diculescu, V. C. Voltammetric determination of all DNA nucleotides. *Anal. Biochem.* **2004**, *332* (2), 321–329. DOI: <https://doi.org/10.1016/j.ab.2004.06.021>.
49. Romero, E.; D’Vries, R.; Zuluaga, F.; Chaur, M. Multiple dynamics of hydrazone based compounds. *J. Braz. Chem. Soc.* **2015**, *26* (3) 1255-1273. DOI: <https://doi.org/10.5935/0103-5053.20150092>.

Article citation:

Martínez, G.; Zuluaga, F.; Chaur, M. N. Electrochemical properties of grid-type metal ion complexes (Fe²⁺ and Co²⁺) with a pyridine-pyrimidine-pyridine based bis(hydrazone). *Rev. Colomb. Quim.* **2018**, *47* (2), 45-53. DOI: <https://doi.org/10.15446/rev.colomb.quim.v47n2.66081>.